Vol 17 No 4, April 2008
1674-1056/2008/17(04)/1291-07

Chinese Physics B

© 2008 Chin. Phys. Soc.
and IOP Publishing Ltd

Linear and nonlinear optical properties of ZnO nanorod arrays

Xiao Si(肖 思)[a)], Su Xiong-Rui(苏雄睿)[a)], Li Chun(李 春)[a)],
Han Yi-Bo(韩一波)[a)], Fang Guo-Jia(方国家)[a)b)], and Wang Qu-Quan(王取泉)[a)b)†]

[a)] *Department of Physics, Wuhan University, Wuhan 430072, China*
[b)] *Key Laboratory of Acoustic and Photonic Materials and Devices of Ministry of Education, Wuhan University, Wuhan 430072, China*

(Received 24 April 2007; revised manuscript received 17 August 2007)

Polarization-dependent linear absorption, second-harmonic generation (SHG) and 3rd-order nonlinearities of well-aligned ZnO nanorod arrays have been investigated with ps pulses. The depressed spectral width and the enhanced intensity of reflective SHG along the long axis of ZnO nanorods were observed by using p-polarized pulses, which is explained by the optical confinements. The nonlinear absorption coefficient measured with s-polarization reached the maximum 4.0×10^4cm/GW at the wavelength $\sim$750 nm, which revealed a large two-photon resonance absorption attributed to the quantum confined exciton when the polarization is vertical to the long axis of ZnO nanorod.

Keywords: ZnO, nanorods, second-harmonic generation, nonlinearity
PACC: 4265K, 6146

1. Introduction

Zinc oxide is a remarkable wide band-gap semiconductor with diverse properties such as ultraviolet (UV) emission,[1,2] transparent conductivity,[3] and piezoelectricity.[4] One-dimensional (1D) ZnO nanocrystals exhibit the most abundant configurations of nanostructures,[5−7] and have a wide range of promising applications in UV photonic devices,[8] field emission devices,[9,10] sensors,[11] and piezoelectric nanogenerators.[12]

ZnO nanorods (NRs) have both optical and quantum confinements, which are very importance for their applications in photonic devices. The optical confinement of the aligned NR arrays leads to better optical emitting and propagating properties and results in UV lasing along the long axis of the aligned NRs.[13,14] Besides the large optical nonlinearity due to the unequal atomic size of Zn and O and the polar potentials of ZnO crystal,[15,16] the enhanced second-harmonic-generation (SHG) and other enhanced nonlinear processes by the resonant two-photon absorption to the exciton level in ZnO NRs and films are also reported.[17]

In this Letter we investigate polarization-dependent linear absorption and refraction, second-harmonic generation (SHG) and 3rd-order nonlinearities of well-aligned ZnO NRs. To analyse the enhancement mechanism of nonlinearity, the spectral responses of SHG and the nonlinear absorption are also involved.

2. Experiments

Vertically well-aligned ZnO NR arrays were grown on a ZnO film coated quartz substrate by using a hydrothermal process. The ZnO film seed layer was deposited on quartz in a pulsed laser deposition (PLD) system. The deposition details of the ZnO film have been described elsewhere.[18] After seeded, the substrate was placed in an aqueous solution of zinc nitrate hydrate ($Zn(NO_3)_2{\cdot}6H_2O$, 0.05 mol/L) and hexamethylenetetramine (HMT, 0.05 mol/L). The aqueous solution is kept in a Teflon-lined stainless-steel autoclave at 80°C for 5 h. After that, the sample was taken out, rinsed in flowing de-ionized water immediately and blown dry with N_2 gas.

†Corresponding author. E-mail: qqwang@whu.edu.cn

The as-synthesized ZnO nanostructures were characterized by field emission scanning electron microscopy (FE-SEM, Philips XL30), x-ray diffraction spectrum (XRD, Bruker D8 Advance). The absorption spectra measurements were carried out using an UV–VIS–NIR spectrophotometer (Varian, Cary 5000). The SHG signals were detected by a cooled CCD detector (SPEC-10, Princeton) through a monochromator (Spectrapro 2500i, Acton). The nonlinear absorption was investigated by using Z-scan technique. The excitation light source was a mode-locked Ti: sapphire laser (Coherent Mirra 900) at 2ps pulse width and 76MHz repetition rate. The polarized direction of the input beam was controlled by a half-wave plate which was put before the sample.

3. Results and discussion

The scanning electron microscope (SEM) images of the ZnO NR arrays are shown in Figs.1(a) and 1(b). The NRs are vertically aligned well on the substrate. They have diameters from 30 to 100 nm and lengths of about 500 nm. The images also show that the rods are solid and dense over a broad area on the substrate, arranged roughly parallel to one another. The average spacing between the NRs ranges form 30 to 50 nm. The strong (002) peak as well as other weak peaks at a diffraction angle (2θ) of 34.5° in the XRD patterns indicates that ZnO NRs had a wurtzite structure (see Fig.1(c)).

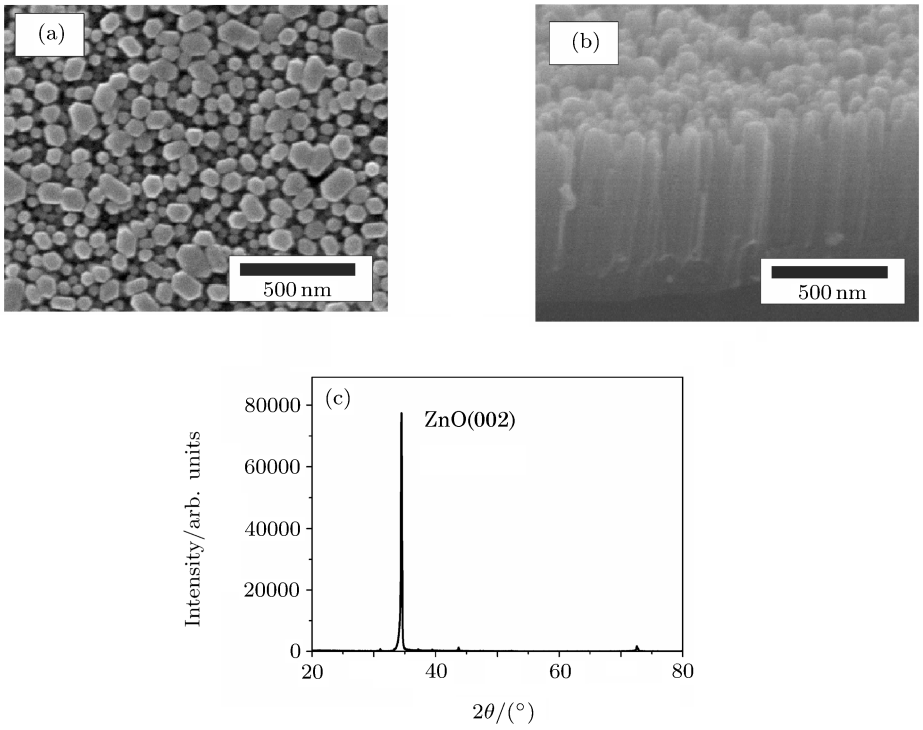


Fig.1. Nanostructure of ZnO NR arrays. (a) Top view SEM image, (b) cross section SEM image, (c) XRD pattern.

The transmittance and the reflection of the ZnO NR arrays versus polarization angle were measured at the incident angle $\theta_{\rm in}$=45°, as shown in Fig.2(a). The polarization angle $\theta_{\rm s}$ was adjusted by a $\lambda/2$ wave-plate; $\theta_{\rm s}$ equals 0 and $\pi/2$ for the s- and p-polarization light, respectively. The reflectivity R decreases and the transmittance T increases with increasing $\theta_{\rm s}$ (see Fig.2(b)). The shape of $R-\theta_{\rm s}$ curve of the aligned ZnO NR sample is similar to the ZnO film, but the R value of the NR sample is smaller than that of the film due to the relative smaller effective dielectric function. The pure absorption α of the sample is calculated from the measured transmittance and the reflectivity by using the relationship $\alpha L = -\ln(T/(1-R))$. Figure 2(c) shows that the pure absorption α of the aligned ZnO NRs decreases with increasing $\theta_{\rm s}$. The ratio $\alpha(\theta_{\rm s}=0)/\alpha(\theta_{\rm s}=\pi/2)$ equals 1.36 at the wavelength 780 nm. The NR sample exhibits a larger linear

absorption when the polarization of the light is vertical to the long axis of the ZnO NRs, which may be caused by the surface defect[19] and the quantum confinement effect of the ZnO NRs.[20]

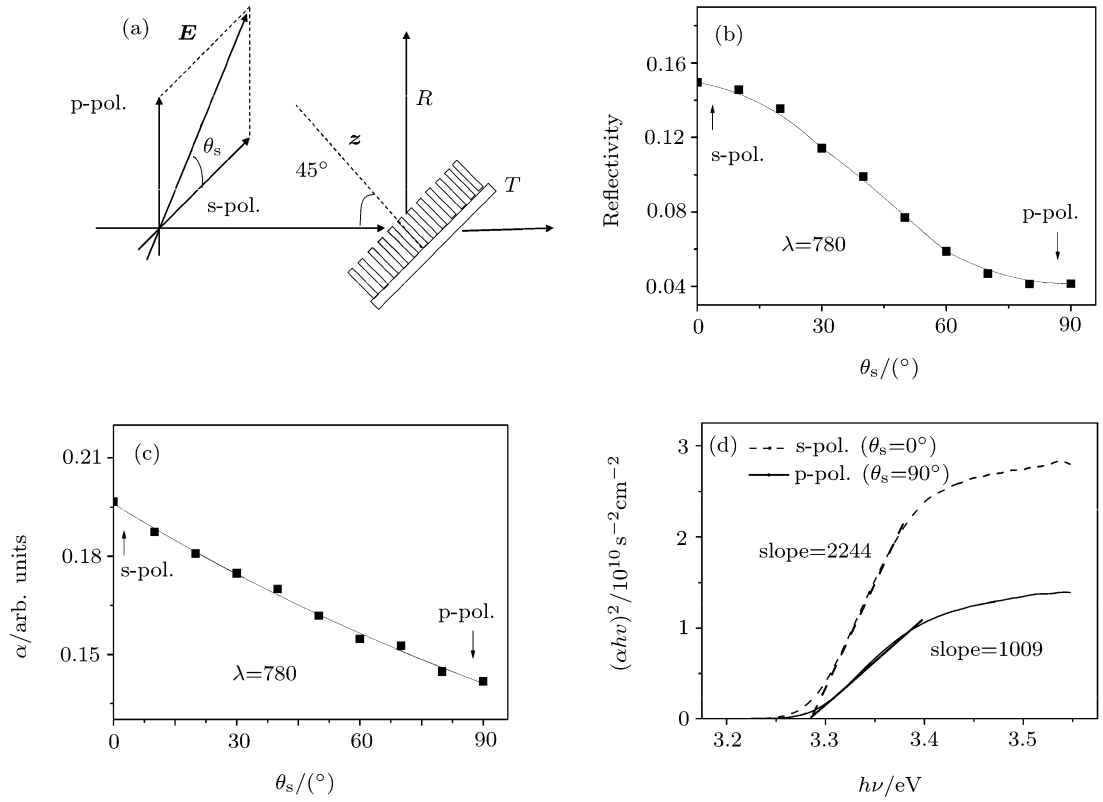


Fig.2. Linear optical absorption properties. (a) The measuring method and the incident angle θ_{in} 45°. (b) The reflectivity vs. θ_s. (c) The effective attenuation efficient α_{eff} vs. θ_s. (d) Plot of $(a_0E_{phot})^2$ versus E_{phot} for direct transition at θ_s=0° and 90°, band gap energy E_g obtained by extrapolation to a_0=0.

The absorption spectra near the band edge with s- and p-polarization light are shown in Fig.2(d). It clearly shows that the absorption near the band edge with s-polarization increases much fast than that with p-polarization, but the difference of the band gap energy E_g is very small for the two different polarizations. The dashed fitting lines near the band edge in Fig.2(d) has the exponential form:[21]

$$(\alpha h\nu)^2 = A^{*2}(h\nu - E_g), \tag{1}$$

where hv is the photon energy, the value of A^{*2} is equal to the slope of the fitting line in Fig.2(d). Notice that the effective refractive index n_{eff} of the sample is proportional to $1/A^*$,[22] so, a larger slope in $(\alpha h\nu)^2 - h\nu$ curve represents a smaller effective refractive index n_{eff} when the polarization of the light is vertical to the long axis of the ZnO NRs. The measured ratio $n_{eff}(\theta_s = \pi/2)/n_{eff}(\theta_s$=0)=$A^*(\theta_s$=0)/$A^*(\theta_s = \pi/2)$ is about 1.49.

Two facts lead to the results $n_{eff}(\theta_s = \pi/2) > n_{eff}(\theta_s$=0). One is that $n_{ZnO}(||) > n_{ZnO}(\perp)$,[23,24] where n_{ZnO} is the refractive index of the ZnO NR, the symbols '||' and '$\perp$' represent the polarization is parallel and vertical to the long axis of the NRs, respectively. Another is that $\varepsilon_{eff}(||) > \varepsilon_{eff}(\perp)$, where $\varepsilon_{eff} \approx n_{eff}^2$ represents the effective dielectric function of the well-aligned ZnO NRs, which can be calculated from the formula

$$\frac{\varepsilon_{eff} - \varepsilon_{Air}}{\varepsilon_{Air} + L(\varepsilon_{eff} - \varepsilon_{Air})} = f_{ZnO}\frac{\varepsilon_{ZnO} - \varepsilon_{Air}}{\varepsilon_{Air} + L(\varepsilon_{ZnO} - \varepsilon_{Air})}, \tag{2}$$

where ε_{Air} and ε_{ZnO} are the dielectric function of air and the ZnO NRs, respectively; f_{ZnO} represents the volume fraction of the ZnO NRs in the composite film, which is estimated to be about 0.80 from the SEM images shown in Figs.1(a) and 1(b). L is the depolarization factor of the ZnO NRs, which equals 0 and

1 when the polarization is vertical and parallel to the long axis of the NRs, respectively. Equation (2) gives two fundamental relations,

$$\varepsilon_{\text{eff}}(\perp) = f_{\text{ZnO}}\varepsilon_{\text{ZnO}}(\perp) + (1 - f_{\text{ZnO}})\varepsilon_{Air}, \quad L = 0, \quad (3)$$

$$\varepsilon_{\text{eff}}^{-1}(\|) = f_{\text{ZnO}}\varepsilon_{\text{ZnO}}^{-1}(\|) + (1 - f_{\text{ZnO}})\varepsilon_{\text{Air}}^{-1}, \quad L = 1. \quad (4)$$

From Eqs.(3) and (4), the $n_{\text{eff}}(\|)/n_{\text{eff}}(\perp)$ calculated is about 1.28 when $n_{\text{ZnO}}(\perp) = n_{\text{ZnO}}(\|) = 2.2$.

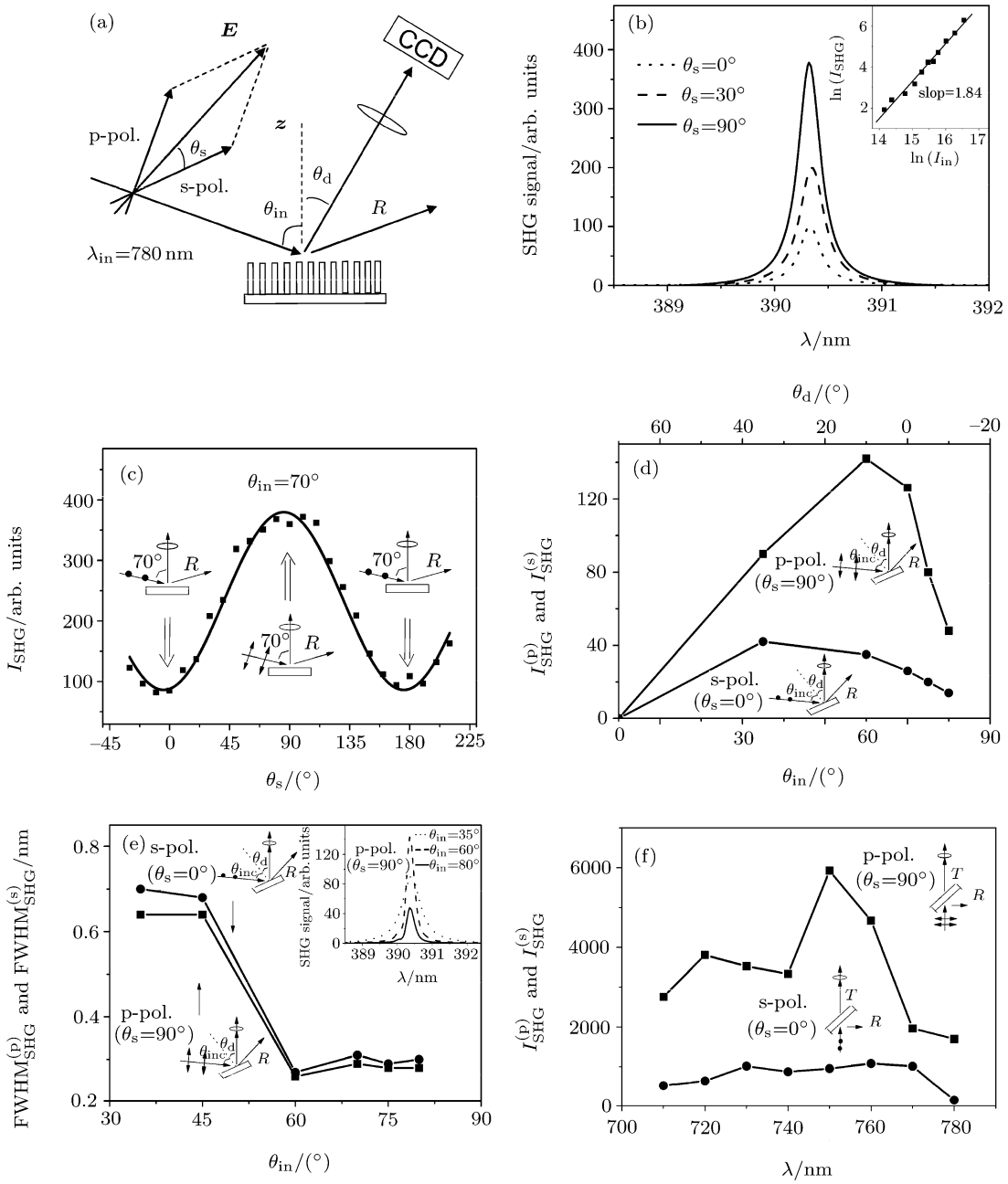


Fig.3. Second-order optical properties. (a) The SHG measuring method and the exciting wavelength 780 nm, at $\theta_{\text{in}}+\theta_{\text{d}}=70°$. (b) The measured SHG curves at $\theta_{\text{s}} = 0°$, 30° and 90°, for $\theta_{\text{in}}=70°$ and $\theta_{\text{d}}=0°$. The inset is the I_{SHG} of the ZnO NR arrays as a function of I_{in}. (c) The SHG intensity I_{SHG} vs. θ_{s}. (d) The SHG intensity vs. θ_{in}. The squares and dots correspond to the p-polarized and s-polarized fundamental beams, respectively. (e) The ratio of I_{SHG} (p-pol.) and I_{SHG} (s-pol.) vs. θ_{in}. (f) The FWHM of SHG sign vs. θ_{in}. The squares and dots correspond to the p-polarized and s-polarized fundamental beams, respectively. The inset is the measured SHG curve at θ_{in} =30°, 60° and 80° for the p-polarized fundamental beam. (f) The SHG intensity vs. the exciting wavelength.

To investigate the 2nd-order optical nonlinearity of the ZnO NRs, the SHG was investigated. The excitation polarization dependence on SHG of ZnO NR sample was measured at the excitation wavelength λ_{exc}=780 nm, which is off resonance to the two-photon absorption at the exciton level (∼753 nm) and the band edge (∼730 nm). The dominant origination of SHG is the crystal structure, not the quantum effect in this case. The geometry to record reflective SHG is illustrated in Fig.3(a), in which, the incident angle θ_{in} is 45°, and the emission angle θ_d between the long axis of the aligned NRs and the detection direction is 25° ($\theta_{in}+\theta_d$=70°). The slope of the logarithmic plots of the SHG intensity I_{SHG} versus laser power I_{in} is about 1.84 (see the inset of Fig.3(b)), which indicates that the SHG is generated by two-photon absorption process. The measured SHG signals with polarization angles θ_s=0°, 30° and 90° are shown in Fig.3(b).

The SHG intensity of the ZnO NR arrays varies with the excitation polarization angle θ_s (see Fig.3(c)), it reaches the minimum at θ_s=0° (s-polarization). SHG intensity excited by p- and s-polarization are expressed by I_{SHG}(p) and I_{SHG}(s), respectively, and the ratio I_{SHG}(p)/I_{SHG}(s) is about 4.4 at λ_{exc}=780 nm. The 2nd-order nonlinearity (SHG) of the NR arrays is strongly suppressed due to the symmetry of the cross-section of the NRs when the polarization of the excitation field is vertical to the long axis of the aligned NRs (θ_s=0°, s-polarization).[25]

The SHG intensity of ZnO NR arrays is strongly dependent on the incident angle θ_{in} and the emission angle θ_d due to the optical confinement. The recording geometry is the same as that shown in Fig.3(a), $\theta_{in}+\theta_d$=70° and λ_{exc}=780 nm. The ratio I_{SHG}(p)/I_{SHG}(s) is larger than 1 in the whole range of incident angle θ_{in} (or emission angle θ_d) as shown in Fig.3(d). The SHG signal I_{SHG}(s) excited with s-polarized pulses reaches the maximum at $\theta_{in}=\theta_d$=35°, meaning a large collection efficiency of SHG along the reflecting direction, which is similar to the measured results of thin film and bulk. The SHG signal I_{SHG}(p) excited with p-polarized pulses exhibits quite different behaviours: the SHG peak intensity increases from 0 to the maximum 140, and the SHG spectral width decreases from 0.68 nm to the minimum 0.27 nm, when the emission angle θ_d decreases from 70° to 10° (see Figs.3(d) and 3(e)). These lasing behaviours of SHG emissions along the long axis of aligned ZnO NRs are caused by the optical confinement of the NRs. The sharp UV emissions or lasing from the aligned ZnO NRs and GaN NRs have been widely reported,[13,26] but the lasing behaviours of SHG emissions are reported for the first time in this work, so far as we know.

To investigate the enhanced SHG caused by the nonlinear absorption and its emission dynamics, the transmittance SHG signals were recorded in the excitation photon energy range 1.59 eV(780 nm)–1.72 eV(720 nm) as shown in Fig.3(f), and the incident angle θ_{in} is set at 45°. The maximal SHG peak intensity is observed by using p-polarized pulses at the excitation wavelength 750 nm. Since the wavelength 750 nm is corresponding to the resonant two-photon absorption on the exciton level of the ZnO NRs, it implies a relatively stronger quantum confinement of the excitons in ZnO NRs with a small diameter when the polarization is vertical to the long axis of the ZnO NRs.

The nonlinear absorption coefficient β of the aligned ZnO NRs was measured by open-aperture Z-scan, which corresponds to the imaginary part of the third-order optical susceptibility. Figure 4(a) illustrates the geometry for the Z-scan measurements at an incident angle 45°. The recorded open-aperture Z-scans can be theoretically fitted with the formula,[27]

$$T_{OA} = \sum_{m=0}^{\infty} \frac{(-q_0)^m}{(1+z^2/z_0^2)^m(1+m)^{3/2}}, \quad (m \geq 0) \quad (5)$$

where T_{OA} is the normalized transmittance, z is the distance of the sample from the focal position and z_0 is the Rayleigh length of the laser beam; $q_0 = \beta I_0 L_{eff}$, with I_0 being the irradiance of the laser beam at the focus (z=0) and $L_{eff} = [1-\exp(-\alpha_0 L)]/\alpha_0$ is the effective thickness of the film ($L \approx$707 nm). The recorded $T_{OP}(z)$ curves of ZnO aligned NRs are shown in Fig.4(b). From the Z-scan measurements at a wavelength 780 nm, we obtained $\beta(\theta_s = 0°)$=2.21×10^4 cm/GW, $\beta(\theta_s = 90°)$=2.08×10^{4}cm/GW.

The spectral responses of the nonlinear absorption of the ZnO NR arrays are shown in Fig.4(c). Notice that β (at $\theta_s = 0°$) reaches the maximum at a wavelength 750 nm, which is attributed to the two-photon resonance absorption of excitonic states; but β (at $\theta_s = 90°$) reaches the maximum at a wavelength 730 nm, which is attributed to the two-photon resonance absorption of the band edge.[19] We can see that $\beta(\theta_s = 0°)/\beta(\theta_s = 90°)$ reaches 1.36 at the wavelength 750 nm, meaning a stronger two-photon resonance absorption of excitonic states when the polarization is vertical to the long axis of the ZnO NRs.

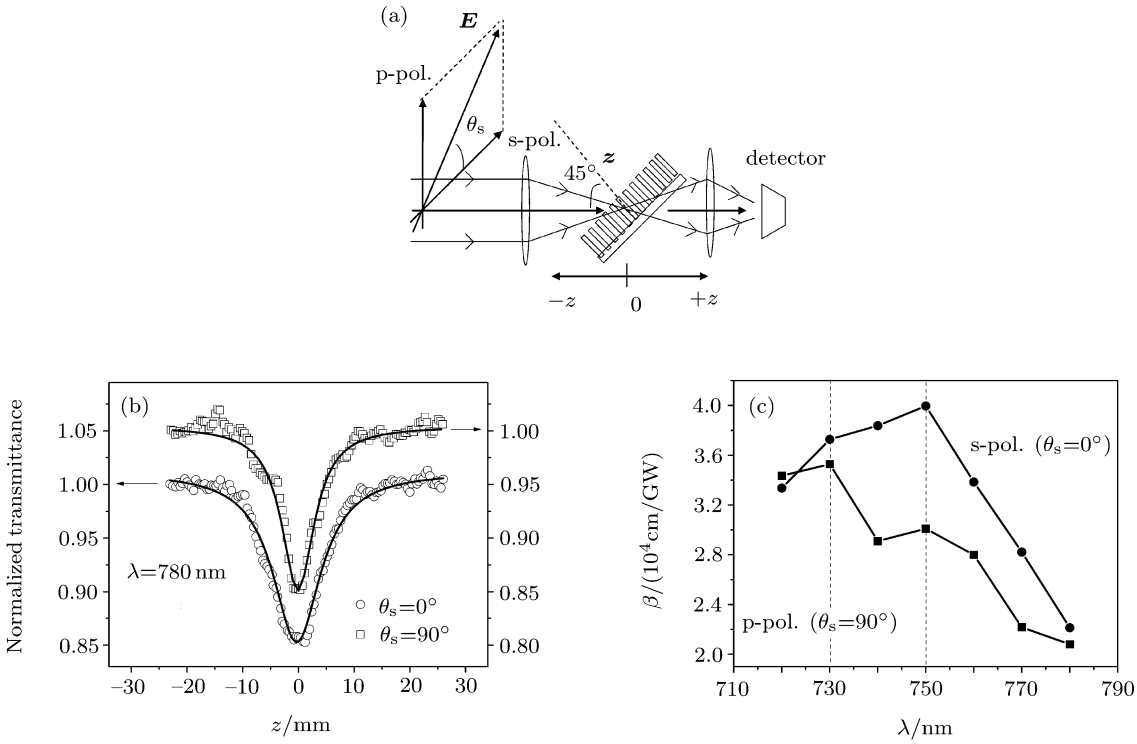


Fig.4. Third-order optical properties. (a) The arrangement of a special z-scan measurement at an incident angle $\theta_{\rm in}$ 45°. (b) The measured open-aperture z-scan curve at $\theta_{\rm s}$=0° and 90° with the exciting wavelength 780 nm. (c) The nonlinear absorption coefficient β vs. the exciting wavelength. The squares and dots correspond to the p-polarized and s-polarized fundamental beams, respectively.

4. Conclusion

The SHG intensity and nonlinear absorption coefficient of the aligned ZnO NRs have been measured with s-polarization and p-polarization of the laser. A maximal SHG peak intensity is observed by using p-polarization pulses; its spectral width is depressed and peak intensity is enhanced when the SHG emits along the long axis of the ZnO NRs. These behaviours can be explained by the cavity effect of the aligned NRs. The maximal nonlinear absorption coefficient is obtained by using s-polarization pulses at the wavelength 750 nm, which is attributed to the two-photon resonant absorption of the exciton level of the ZnO NRs. The observations reported here may be helpful to understand the intrinsic relations of the linear and nonlinear optical processes in the ZnO NRs.

References

[1] Servce R F 1997 *Science* **276** 895

[2] Sun H, Zhang Q F and Wu J L 2007 *Acta Phys. Sin.* **56** 3479 (in Chinese)

[3] Kulkarni A J and Zhou M 2006 *Appl. Phys. Lett.* **88** 141921

[4] Kong X Y and Wang Z L 2003 *Nano. Lett.* **3** 1625

[5] Li J Y, Chen X L, Wei Z F and Qiao Z Y 2001 *Chin. Phys. Lett.* **11** 1527

[6] Wang F F, Cao L, Liu R B, Pan A L and Zou B S 2007 *Chin. Phys.* **16** 1790

[7] Liu R B, Pan A L, Wang F F and Zou B S 2007 *Chin. Phys.* **16** 1129

[8] Liu D F, Tang D S, Ci L J, Yan X Q, Liang Y X, Zhou Z P, Yuan H J, Zhou W Y and Wang G 2003 *Chin. Phys. Lett.* **20** 928

[9] Lee C J, Lee T J, Lyu S C, Zhang Y, Ruh H and Lee H J 2002 *Appl. Phys. Lett.* **81** 3648

[10] Ni S L, Chang Y Q, Long Y and Ye R C 2006 *Acta Phys. Sin.* **55** 5409 (in Chinese)

[11] Wen Q, Li Q H, Chen Y J, Wang T H, He X L, Li J P and Lin C L 2004 *Appl. Phys. Lett.* **84** 3654

[12] Wang Z L and Song J H 2006 *Science* **312** 242

[13] Johnson J C, Yan H Q and Saykally R J 2003 *J. Phys. Chem.* B **107** 8816

[14] Guenther R D 1999 *Modern Optics* (New York: Wiley)

[15] Levine B F 1970 *Phys. Rev. Lett.* **25** 440

[16] Wang R Y, Wu X C, Zhou B S, Wang L, Wu P F, Liu S M, Wang J G and Xu J R 1998 *Chin. Phys. Lett.* **1** 27

[17] Prasanth P R, Vugt L K, D Vanmaekelbergh A M and Gerritsen H C 2006 *Appl. Phys. Lett.* **88** 181501
[18] C Johnson J, Yan H Q, D Schaller R, B Petersen P, Yang P D and J Saykally R 2002 *Nano. Lett.* **2** 279
[19] Srikant V and Clarke D R 1997 *J. Appl. Rhys.* **81** 6357
[20] Gu Y, Kuskovsky Lgor L, Yin M, O'Brien S and Neumark G F 2004 *Appl. Phys. Lett.* **85** 3833
[21] Wang L W and Zunger A 1996 *Phys. Rev.* B **53** 9579
[22] Bardeen J, Blatt F J and Hall L H 1954 *Proc. of Atlantic City Photoconducity Conference* (USA: Wiley and Chapman an Hall) p146
[23] Xi J Q, Kim J K, Schubert E F, Ye D, Lu T M, Lin S Y and Juneja J S 2006 *Opt. Lett.* **31** 601
[24] Xi J Q, Jong K K and Schubert E F 2005 *Nano. Lett.* **5** 1385
[25] Tom H W K, Heinz T F and Shen Y R 1983 *Phys. Rev. Lett.* **51** 1983
[26] Fan Z Y, Cahng P C, Lu J G, Walter E C, Penner R M, Lin C H and Lee H P 2004 *Appl. Phys. Lett.* **85** 6128
[27] Sheik-Bahae M, Said A A, Wei T H, Hagan D J and Stryland E W V 1990 *IEEE. J. Quantum Electron* **26** 760